PUBLICATION IV

Facile Method for Stiff, Tough, and Strong Nanocomposites by Direct Exfoliation of Multilayered Graphene into Native Nanocellulose Matrix

Biomacromolecules 2012, 13 (4), pp 1093–1099,
DOI: 10.1021/bm2018189

Article
pubs.acs.org/Biomac

Facile Method for Stiff, Tough, and Strong Nanocomposites by Direct Exfoliation of Multilayered Graphene into Native Nanocellulose Matrix

Jani-Markus Malho,[†] Päivi Laaksonen,*[,†] Andreas Walther,[‡] Olli Ikkala,[§] and Markus B. Linder[†]

[†]VTT Technical Research Centre of Finland, Tietotie 2, P.O. Box 1000, FI-02044, Espoo, Finland

[‡]DWI at RWTH, Aachen University, Forckenbeckstr. 50, D-52056, Aachen, Germany

[§]Molecular Materials, Aalto University (formerly Helsinki University of Technology), P.O. Box 15100, FI-00076 AALTO, Espoo, Finland

ABSTRACT: Nanofibrillated cellulose (NFC) is a natural fibrillar material with exceptionally high mechanical properties. It has, however, been exceedingly difficult to achieve nanocomposites with drastically improved mechanical properties by dispersing NFC as random networks to polymer matrices, even using compatibilization. We show nanocomposites consisting of aligned assemblies of multilayered graphene and NFC with excellent tensile mechanical properties without any surface treatments. The optimum composition was found at 1.25 wt % graphene multilayers, giving a Young's modulus of 16.9 GPa, ultimate strength of 351 MPa, strain of 12%, and work-of-fracture of 22.3 MJ m^{-3}. This combines high strength with relatively high toughness and is obtained by direct exfoliation of graphite within aqueous hydrogels of NFC where an optimum sonication power is described. The results suggest the existence of an attractive interaction between multilayered graphene flakes and cellulose. Aligned assemblies are obtained by removal of water by filtration. The concept can be beneficial for applications because it results in high mechanical properties by a simple and environmentally green process.

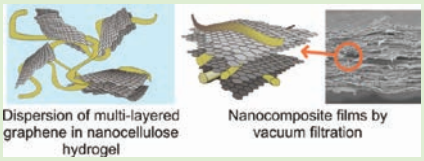

INTRODUCTION

Nature shows several types of nanocomposite materials with excellent properties that are difficult to obtain in conventional manmade composites.[1] Representative examples are pearl of nacre and silk, which are based on aligned assemblies of hard reinforcing and soft dissipative domains, leading to unique combinations of stiffness, strength, and toughness. On the other hand, also wood and plant cell wall materials show remarkable multifunctionality and adaptability due to their reinforcing native cellulose nanofibrils (nanofibrillated cellulose, NFC, also called microfibrillated cellulose, MFC) as hierarchically embedded in soft matrix at controlled pitches.[2] By understanding the essential features of biological materials, improved properties may be designed in synthetic materials. This approach of learning from nature is called biomimetics.[3−9] It involves several scientific challenges but can result in technologically promising materials.[10−15]

Toward biomimetic constructs, macroscopic pulp fibers can be mechanically disintegrated into NFC usually also involving pretreatments,[16−20] which have excellent mechanical properties.[2] These nanofibrils have a width of 5−30 nm and total length up to about 5 μm. They consist of mostly native crystalline cellulose regions separated by short amorphous domains according to the fringed fiber model. Upon disintegration from pulp, NFC usually forms hydrogels.[21] Thus, an efficient and economical exploitation of native NFC involves processing in aqueous environment to limit heavy agglomeration of strongly hydrogen-bonding nanofibrils in nonpolar media. Creating a solid composite from aqueous NFC suspension requires the removal of water, leading to a network structure due to the capillary forces that introduce an attraction between fibrils. Multiple molecular level interactions such as hydrogen bonds bind the nanofibrils together.[22] NFC fibrils are considered one of the most interesting and promising renewable materials for applications such as aerogels,[23,24] nanopaper,[13] fibers,[25,26] composites,[27−30] and other hybrid materials.[31,32]

Graphene[33] is another feasible material for nanocomposites due to its high stiffness and strength.[34,35] Graphene can be produced by micromechanical cleavage,[36] by growth of monolayers of graphene[37,38] or by exfoliation from graphite.[39−42] In addition, some production steps result in graphene derivatives, such as graphene oxide.[43] Production of graphene is still a bottleneck for its efficient large scale utilization, especially for composites. Dispersing graphene effectively in composite materials is expected to enable low-cost solutions[44] for sustainable and lightweight materials. Recently many composites using graphene have been reported, especially with different polymers.[43,45] However, facile and robust techniques

Received: December 21, 2011
Revised: February 27, 2012
Published: February 28, 2012

dx.doi.org/10.1021/bm2018189 | *Biomacromolecules* 2012, 13, 1093−1099

for nanocomposites with superior mechanical properties are still being sought.

We showed recently that graphene can improve the properties of NFC composites.[28] To achieve this, graphene flakes were exfoliated using an adhesive protein called hydrophobin.[46,47] The hydrophobin was genetically modified so that a cellulose binding part was joined to it. In the nanocomposite, the hydrophobin bound to graphene flakes and the cellulose binding part bound to nanofibrillated cellulose, and therefore this bifunctional protein could link the graphene and nanocellulose in the nanocomposite material. The linkage resulted in an increase in especially the stiffness and ultimate strength. The importance of the protein linkage to cellulose was shown by using also hydrophobin without the cellulose binding part, which resulted in much weaker materials.

Here we show that a strong, stiff, and tough sheet/fiber-nanocomposite based purely on graphene multilayers and NFC using a sonication process can be made. The work was based on the serendipitous finding that multilayers of graphene can be exfoliated directly from graphite to aqueous environment by using only NFC as the dispersing agent. Our lightweight nanocomposite introduces superior mechanical properties by some forms of physical interaction between NFC fibrils and graphene flakes, to be discussed later. The resulting aqueous suspensions were then vacuum filtrated to form solid composite materials. For simplicity, the dispersions of single or multilayered graphene flakes are referred here as graphene dispersions, although there may be a range of flake thicknesses present. Remarkable improvements were observed in the mechanical properties in comparison to previous results reported on nanopaper and graphene nanocomposite materials.[21,29,48,49] We suggest that the physical interaction between NFC and graphene multilayers generates the basis for the excellent mechanical properties and highlights a novel way for graphene exfoliation.

EXPERIMENTAL SECTION

Material and Methods. *Exfoliation of Graphene Flakes.* A dilute hydrogel (solid content 1.9%) of UPM Fibrillar Cellulose (NFC; UPM-Kymmene Corporation, Finland) was used for graphene exfoliation. The sample preparation was done using mechanical disintegration of birch pulp by ten passes through a M7115 Fluidizer (Microfluidics Corp., U.S.A.) essentially according to previous reports.[19]

Powder of Kish graphite (Natural Kish Graphite (Grade 50), Graphene Supermarket, U.S.A.) was directly exfoliated to graphene flakes using a tip sonicator (Vibra-Cell VCX 750, 2 mm stepped microtip, Sonics and Materials Inc., U.S.A.). Sonication time was based on the amount of energy lead to the sample, which was monitored during the sonication using 60% of the full output power. Graphite granules were predispersed into a NFC solution (2.0 g L^{-1}), creating dispersion with relatively high concentration of graphene flakes, from which smaller amounts of graphene flakes could be dosed for further sonication. Thus, the amount of graphene that is reported, means the whole range of flakes containing single or several layers of graphene.

Preparation of Films. All of the suspensions and diluted dispersion were less than 3.5 mL in volume, because of the high viscosity of NFC lead to inefficient sonication of larger volumes. Graphene suspension having 1.0 g L^{-1} concentration of graphene and 2.0 g L^{-1} of NFC was first exfoliated with 6 kJ of energy. After exfoliation, the desired proportions of graphene/NFC dispersions were prepared by mixing with NFC suspension using sonication energy of 2.5 kJ. The NFC concentration was kept 2.0 g L^{-1} throughout the manufacturing process. Vacuum filtration was used to create the films from dispersions containing NFC and graphene multilayers. The dispersions were filtrated using a Durapore membrane (GVWP, 0.22 μm, Millipore, U.S.A.). After filtration of the films a gentle press was applied to them using a 300 g load for 10 min to prevent wrinkling. Films were dried overnight in +65 °C.

Mechanical Testing. A mini tensile tester (Deben, UK) was used to perform mechanical tests. A 20 N load cell was used with a nominal strain rate of 0.5 mm/min, because of its optimal data range. At least 4 specimens were measured from each sample. Specimen sizes were 2 cm × 2 mm × 7−10 μm, length, width, and thickness, respectively. Mechanical testing was done in ambient conditions.

Characterization of the Samples. Micrometer slide calliper and optical microscope (LEO1560, Carl Zeiss Inc., U.S.A.) were used to determine the widths of the samples. The thicknesses were measured using scanning electron microscope (JEOL JSM-7500F FEG, Japan), where acceleration voltages of 1−15 kV were applied and varied depending on the sample. Samples for SEM imaging were sputtered with Pd to enhance imaging conditions and prevent the charging of a sample. Films were aligned perpendicular to the electron beam. The thickness of a film was determined by taking at least eight measures from different places of a film cross section. Graphene multilayers/NFC dispersions were characterized with JEOLS JEM-3200FSC Cryo-Transmission Electron Microscope. Specimens were vitrified on c-flat grids for cryo-imaging using a vitrobot (FEI, U.S.A.). Electron diffraction was measured with a TEM using a selected area aperture at diffraction mode (Tecnai 12, U.S.A.) instrument operating at a 120 kV accelerating voltage.

Raman Microscopy on the Composite Films. Composite films were characterized by confocal Raman microscopy (WITec Alpha 300 RA, Germany) with a 532 nm laser. By monitoring the intensity of the G band at 1544−1649 cm^{-1} or the D′ band at 2644−2812 cm^{-1}, pieces of multilayered graphene and graphite could be easily located. Weak Raman bands at 1097 and 1107 cm^{-1} were associated with crystalline cellulose.[50]

RESULTS

NFC Matrix and Exfoliation of Graphene. The effect of the ultrasonication of NFC was studied first to see whether sonication causes the degradation of NFC fibrils. Therefore cellulose hydrogels were sonicated with different sonication energies, water was removed by filtration to prepare nanopapers and nanopaper mechanical properties were investigated using the sample size of about 2 mL aqueous suspension of NFC using a concentration of 2.0 g L^{-1}. A small sonication energy, ca. 6 kJ, was needed to open the NFC aggregates to reach a sufficient homogeneity of the NFC dispersion which resulted in rather high stiffness of 11.2 GPa and strength of 287 MPa. However, sonication energies higher than 6 kJ, (tested with 12 kJ and 18 kJ) did lead to a lower tensile strength and modulus values, 6.9 GPa and 190 MPa respectively.

It was serendipitously found that if graphite was added in the above-described procedure, the NFC did promote exfoliation of the graphite. A range of nominal amounts of graphite was used up to weight fraction of 50 wt % versus the weight of NFC. Sonication by 6 kJ was sufficient to disperse the graphite as an apparently homogeneous aqueous suspension into the NFC matrix. The suspensions of multilayered graphene flakes exfoliated in NFC hydrogels were found to be relatively stable, regardless of the amount of graphene, as no clear sedimentation was observed even after few months. A cryogenic transmission electron microscopy (cryo-TEM) image of a multilayered graphene flake embedded in a NFC matrix is shown in Figure 1a. The image was taken from a thin film of a vitrified suspension in cryogenic conditions, thus, the native state of the NFC fibrils and the multilayered graphene flakes were essentially preserved without further aggregation. The micrograph shows that graphite is indeed exfoliated to thin flakes consisting of only a few layers of carbon. In addition, the NFC

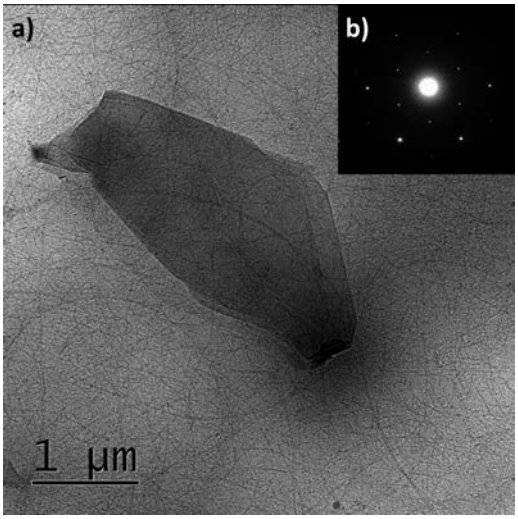

Figure 1. (a) Cryo-TEM image of exfoliated multilayered graphene flake embedded in NFC hydrogel. (b) Electron diffraction pattern of a typical multilayered graphene flake in a NFC matrix.

fibrils are spread homogeneously around the flakes, showing no aggregation due to the presence of the graphitic material. In Figure 1b, a typical electron diffraction pattern, showing the characteristics of a multilayered graphene is presented.

Characterization of NFC/Multilayered Graphene Nanocomposites. Solid composite materials from the aqueous suspensions containing different mass fractions of graphene were formed by removing water from suspensions by vacuum filtration. SEM images of the resulting nanocomposite materials are presented in Figure 2a,b. A cross-sectional image of a nanocomposite containing 50 wt % of graphene is shown in Figure 2b, wherein platelets of multilayered graphene are observed. Figure 2a shows the cross-section of a pure NFC nanopaper, where homogeneous structure of NFC fibrils was observed. In Figure 2b, the composite containing multilayered graphene flakes, shows slightly rougher and more porous structure. The NFC fibrils standing out at one side of the NFC nanopaper are a result of the vacuum filtration. The translucency of the nanocomposite of 1.25 wt % of graphene is shown in Figure 2c, a colored pattern can be seen relatively clearly from beneath of an approximately 10 μm nanocomposite. Figure 2d exhibits the flexibility of the nanocomposite (1.25 wt % graphene) where tweezers were used to fold the nanocomposite without any visible damage or signs of defects.

The thickness and distribution of the graphene flakes were studied by mapping the composite surfaces by Raman microscopy (Figure 3). A random assembly of thin graphite and multilayered graphene flakes was observed. Raman spectra measured at several spots on the composite surface show the characteristic bands of crystalline graphite and graphene multilayers, verifying that graphite was indeed dispersed as thin flakes having lateral dimensions in the micrometer scale.[51] Examples of Raman maps of the graphite main bands measured from the surface are presented in Figure 3b,c. In Figure 3b, a map showing the intensity of the G band is presented, whereas Figure 3c shows the intensity of the D′ band at the same area. The maps show slightly different patterns, indicating differences in flake thickness along the studied region. Example spectra measured at selected spots are presented in Figure 3d. A Raman signal of cellulose near 1095 cm^{-1} was also observed.

Mechanical Properties of NFC/Multilayered Graphene Nanocomposites. Nanocomposites with different amounts of graphene were prepared and their mechanical properties were investigated in tensile mode to find the optimum combination

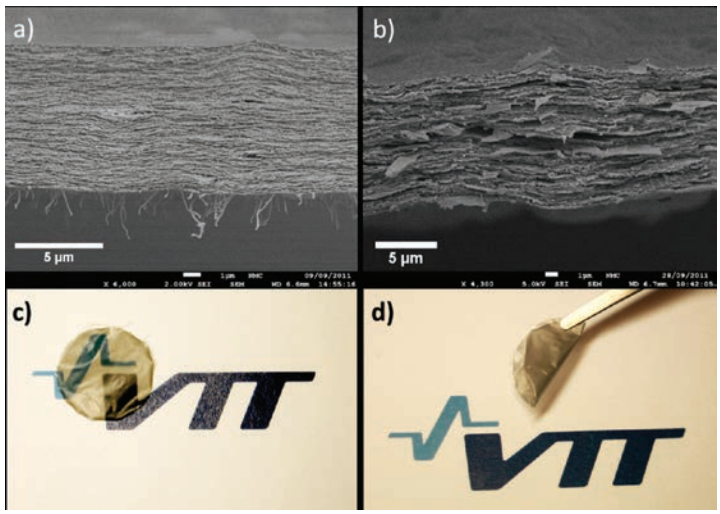

Figure 2. (a) Cross-sectional SEM image of a pure NFC-nanopaper film. (b) Cross-sectional SEM image of graphene/NFC nanocomposite with 50 wt % graphene multilayers. (c) Translucent 1.25 wt % graphene/NFC film on top of a colored pattern. (d) The flexibility of the 1.25 wt % of multilayered graphene nanocomposite shown by folding.

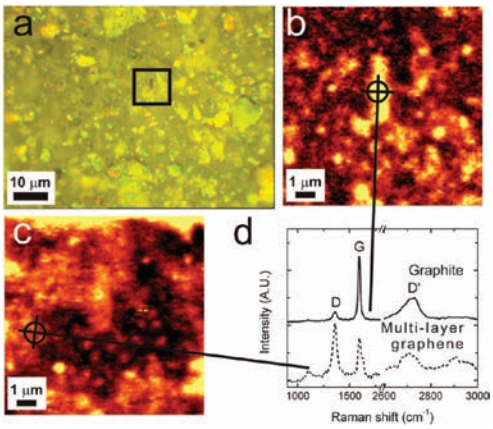

Figure 3. Optical and Raman microscopy images from surface of a film containing 10 wt % of graphene multilayers and NFC. (a) An optical image of the film surface showing flakes of different sizes and thicknesses. (b) Raman map from the highlighted 10 μm × 10 μm area where the intensity of the G band was integrated. (c) Raman map from the highlighted 10 μm × 10 μm area where the intensity of the D′ band was integrated. Raman spectra measured at indicated locations showing characteristic features of graphite (solid line) and a multilayered graphene (dotted line).

of NFC and multilayered graphene. The graphene content (weight percentage, wt %) is given in relation to the amount of NFC. The Young's modulus (Figure 4b), ultimate and yield tensile strength (Figure 4c,d), strain and toughness (Figure 4e,f) obtained from the stress−strain curves show that the optimal performance of the nanocomposite occurred when content of graphene multilayers was 1.25 wt %. At this composition, the properties go through a maximum and beyond this content they start to weaken. At contents of graphene of 5 wt % or more, the properties are even slightly poorer than of pure NFC paper.

Addition of 1.25 wt % of graphene multilayers to NFC results in a significant increase of modulus when compared to pure NFC paper: The measured Young's modulus for 1.25 wt % nanocomposite was 16.9 GPa, while pure NFC paper had a value of 11.2 GPa. Figure 4c,d show the measured ultimate tensile stress and yield stress. In both cases, similar trend as a function of the graphene content could be observed. The highest measured values were 351 MPa for the ultimate tensile strength and 107 MPa for the yield strength. Yield strength was determined from the point at the stress−strain curves where the slope drastically changes and is a measure of the strength that the material can take before plastic deformations start to occur. Changes in the ultimate tensile strength were more drastic than in the yield strength. Yield strength of the composites containing more than 5 wt % of graphene multilayers remained close to the value of pure NFC.

The strain values of the composites containing different amounts of graphene are presented in Figure 4e. The results show that the relative strain did not change much when the graphene content was increased and remained between 10 and 11%. Work-of-fracture, a measure of toughness, is shown for composites having different graphene content in Figure 4f. Again, the highest value was observed at the 1.25 wt % of graphene multilayers, in which the work of fracture reaches 22.3 MJ m^{-3}.

DISCUSSION

By choosing sonication energy properly, NFC nanopaper with remarkably high mechanical performance was first obtained. The tensile strength and work-of-fracture of the pure NFC paper, 287 MPa and 18.9 MJ m^{-3}, respectively, as a combination were among the highest ever reported for nanopaper made from native NFC.[48] Cellulose nanopapers have been reported already before[21] showing tensile strength of 232 MPa and Young's modulus of 13.4 GPa.[29] Our results highlight the importance of optimized conditions for sonication to suppress aggregation to allow thorough fibrillation of NFC. However, the use of excessive mechanical homogenization should be avoided because the properties were clearly deteriorated when sonication was prolonged. Deterioration of the mechanical properties was probably a result of the shortening of fibrils under intensive sonication. The lowering of the degree of polymerization has been shown to significantly affect the mechanical properties of NFC nanopapers.[17,48,52]

We found that NFC hydrogels allow direct exfoliation of graphite without further surface active compounds when using an optimized sonication protocol. The thickness measured for the exfoliated flakes by cryo-TEM, SEM, and Raman microscopy varied from material characterized as bulk graphite to the range of multilayered graphene. Even though bulk graphite was observed by Raman microscopy (Figure 3b), a large fraction of the material embedded in the composite structures showed a relatively strong D′ band, which indicates a material thinner than bulk graphite (Figure 3c).[51] Because the graphene flakes most probably restacked during film formation and compression, localization and identification of single-layer graphene by Raman microscopy was not possible.

Direct ultrasound-assisted dispersion of graphite flakes into NFC matrix is an efficient method for the fabrication of stable and homogeneous dispersions of graphene multilayers in aqueous environment. At low contents, such as 1.25 wt %, the graphene flakes could not be observed from the cross-section of the nanocomposite materials by SEM. The process resulted in an efficient reinforcement of the cellulose nanopaper by a small amount of graphene multilayers. The optimum was observed to be as low as 1.25 wt % of graphene multilayers in a NFC matrix. At higher contents, a more uneven distribution of graphene within the composite structures was observed (Figure 2b), which might also play a role in the deterioration of the mechanical properties.

The combination of multilayered graphene and NFC in a nanocomposite resulted in a superior combination of stiffness (50% increase), toughness (work of fracture 18% increase), and strength (22% increase) compared to the corresponding pristine NFC nanopapers. These remarkable properties suggest that the mechanical strength of the composite is improved through interactions that are mediated by binding between graphene and NFC. This type of interaction has not been described before, but we suggest that our data indicate the existence of such interactions. It has been shown earlier that NFC has an amphiphilic nature, which might explain its behavior with hydrophobic graphene in aqueous environment.[53] Use of aqueous NFC hydrogel as dispersant for graphene flakes shows that these interactions occur also in aqueous environment suggesting that coassembly of graphene layers and NFC might be, at least partly, driven by hydrophobic

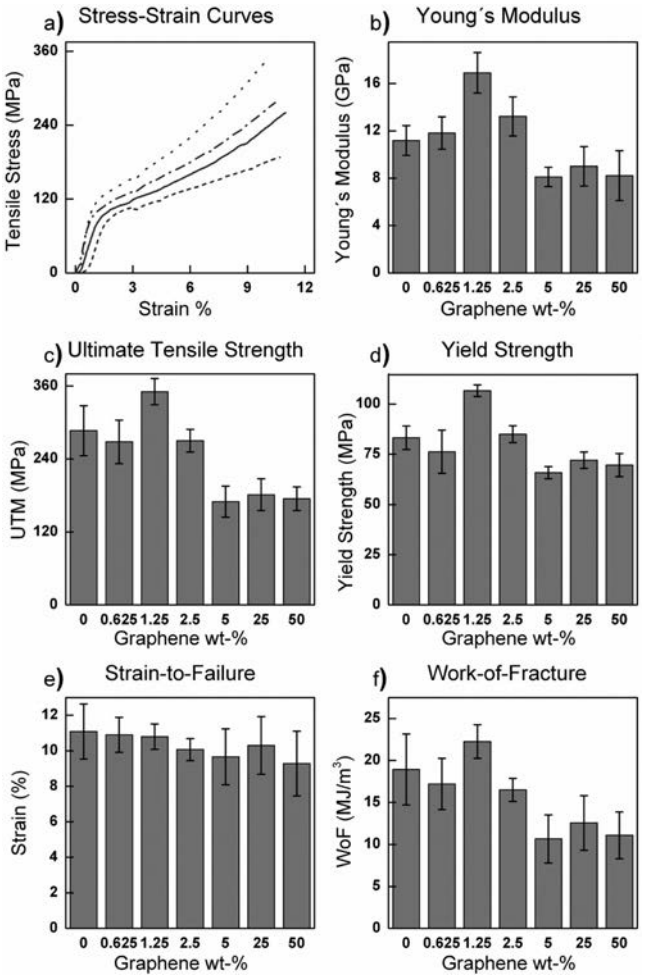

Figure 4. (a) Stress–strain curves of nanocomposites containing NFC and multilayered graphene. The dotted line represents the nanocomposite containing 1.25 wt % of graphene, the dash-dotted line represents the composite containing 2.5 wt % of graphene, the solid line represents pure NFC film and the dashed line represents the nanocomposite containing 25 wt % of graphene multilayers. (b) Young's modulus, (c) ultimate tensile strength, (d) yield strength, (e) strain-to-failure, and (f) work-of-fracture of nanocomposites containing NFC and different amounts of graphene multilayers in relation to the mass of NFC. The presented error bars were calculated from the standard deviation of parallel measurements.

interactions. We also suggest that the attachment of graphene and cellulose could be stabilized by π-interactions.[54] Stacking between π-electron systems and carbohydrates have been observed in several protein-carbohydrate interactions including those of binding domains of cellulose degrading enzymes being able to bind to the (110) crystalline face of cellulose I in the ultrasound.[55] Stacking of π-electrons and cellulose chains have also been observed in the binding of cellulose chains in hydrolytic enzymes.[56,57] This, and the large accessible area of both graphene and flexible nanocellulose fibrils, would explain the enhanced mechanical properties.

The composite had a promoted toughness, appearing especially as high strain-to-failure value even when the composite was stiffened by a significant amount of graphene. The high strain values are likely due to noncovalent bonding between multilayered graphene flakes and the NFC fibrils, allowing them to slide against each other also while NFC fibrils are allowed to slide against each other. During the sliding, the energy could be dissipated by regeneration of hydrogen bonds between NFC fibrils. The sliding of the long fibrils may also lead to their reorientation, which was observed as slight tensile stiffening (Figure 4a). Relative strain values, which were around 10–11% for all of the samples, can be considered as rather high values for composite materials having also high strength and stiffness, since often composite materials become brittle, when they turn stiffer and stronger. Thus, our nanocomposite highlights superior toughness in combination with high strength and stiffness and shows an example of synergistic composite properties.

We previously showed that a protein that binds to both graphene and cellulose could be used to mediate the binding between graphene flakes and NFC and thereby strengthen a nanocomposite material.[32] A comparison between the previous and the present work reveals that the different ways of allowing NFC and graphene interact resulted in materials with distinctly different properties. Most notably the protein aided binding between NFC and graphene flakes led to higher stiffness (20.2 GPa vs 16.9 GPa obtained here) but lower strain to failure (3.1% vs 11% obtained here), and thus lower toughness. The results are easily compared because the same type of NFC was used in both sets of experiments, thus the surface chemistry and surface area were similar, despite the changes in the ultra sound assisted treatment that may have had an effect on the fiber length. We note that using only multilayered graphene and cellulose resulted in a notable increase in stiffness and strength with a largely unaffected strain to failure. Using the protein gave a still markedly higher stiffness, but a clear decrease in strain to failure. The different ways of forming the nanocomposite thus result in very different characteristics in the materials. Apparently the protein is more efficient in forming cohesive binding and may also allow larger parts of the NFC to interact because of the flexible polypeptide linking region in the protein. However, the protein mediated binding seems to allow less flexibility as seen by the lower strain to failure of the protein based material.

CONCLUSIONS

We have shown that graphene multilayers can be directly exfoliated within aqueous hydrogels of native cellulose nanofibrils using sonication without any further additives. Aligned graphene multilayers/NFC nanocomposite assemblies with high modulus, high strength, and work-of-fracture can be achieved by removing water by filtration. The fabrication of the nanocomposite is simple, fast and consumes relatively little energy without production of harmful waste streams, thus it is scalable and supports green pathways. The nanocomposite is generally highly flexible and in the case of 1.25 wt % graphene content it is also partially transparent. An interaction between graphene and NFC is also suggested, showing a rather surprising compatibility of these nanomaterials and their efficient interplay.

AUTHOR INFORMATION

Corresponding Author

*E-mail: paivi.laaksonen@vtt.fi. Fax: +358 20 722 7071. Tel.: +358 20 722 4611.

Notes

The authors declare no competing financial interest.

ACKNOWLEDGMENTS

The Finnish Funding Agency for Technology and Innovation, the Academy of Finland and VTT are thanked for financial support. UPM and The Finnish center for nanocellulose technologies are thanked for their contribution with materials. Suvi Arola is thanked for help with experiments.

REFERENCES

(1) Meyers, M. A.; Chen, P.-Y.; Lin, A. Y.-M.; Seki, Y. *Prog. Mater. Sci.* **2008**, *53*, 1.
(2) Klemm, D.; Kramer, F.; Moritz, S.; Lindström, T.; Ankerfors, M.; Gray, D.; Dorris, A. *Angew. Chem., Int. Ed.* **2011**, *50*, 5438.
(3) Tang, Z.; Kotov, N. A.; Magonov, S.; Ozturk, B. *Nat. Mater.* **2003**, *2*, 413.
(4) Fratzl, P.; Burgert, I.; Gupta, H. S. *Phys. Chem. Chem. Phys.* **2004**, *6*, 5575.
(5) Deville, S.; Saiz, E.; Nalla, R. K.; Tomsia, A. P. *Science* **2006**, *311*, 515.
(6) Munch, E.; Launey, M. E.; Alsem, D. H.; Saiz, E.; Tomsia, A. P.; Ritchie, R. O. *Science* **2008**, *322*, 1516.
(7) Bonderer, L. J.; Studart, A. R.; Gauckler, L. J. *Science* **2008**, *319*, 1069.
(8) Bratzel, G. H.; Cranford, S. W.; Espinosa, H.; Buehler, M. J., *J. Mater. Chem.* **2010**, *20*, 10465−10474.
(9) Antonietti, M.; Fratzl, P. *Macromol. Chem. Physic.* **2010**, *211*, 166.
(10) Takai, O. *Ann. N.Y. Acad. Sci.* **2006**, *1093*, 84.
(11) Sarikaya, M. *Proc. Natl. Acad. Sci. U.S.A.* **1999**, *96*, 14183.
(12) Teeri, T. T.; Brumer, H. 3rd; Daniel, G.; Gatenholm, P. *Trends Biotechnol.* **2007**, *25*, 299.
(13) Andreadis, S. T.; Geer, D. J. *Trends Biotechnol.* **2006**, *24*, 331.
(14) Kowalczyk, S. W.; Blosser, T. R.; Dekker, C. *Trends Biotechnol.* **2011**, *29*, 607.
(15) Walther, A.; Bjurhager, I.; Malho, J.-M.; Pere, J.; Ruokolainen, J.; Berglund, L. A.; Ikkala, O. *Nano Lett.* **2010**, *10*, 2742.
(16) Turbak, A. F.; Snyder, F. W.; Sandberg, K. R. *J. Appl. Polym. Sci.* **1983**, *37*, 815.
(17) Herrick, F. W.; Casebier, R. L.; Hamilton, J. K.; Sandberg, K. R. *J. Appl. Polym. Sci.* **1983**, *37*, 797.
(18) Saito, T.; Kimura, S.; Nishiyama, Y.; Isogai, A. *Biomacromolecules* **2007**, *8*, 2485.
(19) Pääkkö, M.; Ankerfors, M.; Kosonen, H.; Nykänen, A.; Ahola, S.; Österberg, M.; Ruokolainen, J.; Laine, J.; Larsson, P. T.; Ikkala, O.; Lindström, T. *Biomacromolecules* **2007**, *8*, 1934.
(20) Henriksson, M.; Henriksson, G.; Berglund, L. A.; Lindström, T. *Eur. Polym. J.* **2007**, *43*, 3434.
(21) Berglund, L. A.; Peijs, T. *MRS Bull.* **2010**, *35*, 201.
(22) Nakagaito, A. N.; Yano, H. *Appl. Phys. A: Mater. Sci. Process.* **2004**, *78*, 547.
(23) Pääkkö, M.; Vapaavuori, J.; Silvennoinen, R.; Kosonen, H.; Ankerfors, M.; Lindström, T.; Berglund, L. A.; Ikkala, O., *Soft Matter* **2008**, *4*, 2492−2499.
(24) Korhonen, J. T.; Hiekkataipale, P.; Malm, J.; Karppinen, M.; Ikkala, O.; Ras, R. H. *ACS Nano* **2011**, *5*, 1967.
(25) Iwamoto, S.; Isogai, A.; Iwata, T. *Biomacromolecules* **2011**, *12*, 831.
(26) Walther, A.; Timonen, J. V. I; Díez, I.; Laukkanen, A.; Ikkala, O. *Adv. Mater.* **2011**, No. 23, 2924.
(27) Yano, H.; Sugiyama, J.; Nakagaito, A. N.; Nogi, M.; Matsuura, T.; Hikita, M.; Handa, K. *Adv. Mater. (Weinheim, Ger.)* **2005**, *17*, 153.
(28) Nakagaito, A. N.; Yano, H. *Appl. Phys. A: Mater. Sci. Process.* **2005**, *80*, 155.
(29) Sehaqui, H.; Liu, A.; Zhou, Q.; Berglund, L. A. *Biomacromolecules* **2010**, *11*, 2195.
(30) Wang, M.; Olszewska, A.; Walther, A.; Malho, J. M.; Schacher, F. H.; Ruokolainen, J.; Ankerfors, M.; Laine, J.; Berglund, L. A.; Osterberg, M.; Ikkala, O. *Biomacromolecules* **2011**, *12*, 2074.
(31) Czaja, W. K.; Young, D. J.; Kawecki, M.; Brown, R. M. Jr. *Biomacromolecules* **2007**, *8*, 1.
(32) Laaksonen, P.; Walther, A.; Malho, J. M.; Kainlauri, M.; Ikkala, O.; Linder, M. B. *Angew. Chem., Int. Ed.* **2011**, *50*, 8688.
(33) Novoselov, K. S.; Geim, A. K.; Morozov, S. V.; Jiang, D.; Zhang, Y.; Dubonos, S. V.; Grigorieva, I. V.; Firsov, A. A. *Science* **2004**, *306*, 666.
(34) Stankovich, S.; Dikin, D. A.; Dommett, G. H.; Kohlhaas, K. M.; Zimney, E. J.; Stach, E. A.; Piner, R. D.; Nguyen, S. T.; Ruoff, R. S. *Nature* **2006**, *442*, 282.
(35) Geim, A. K.; Novoselov, K. S. *Nat. Mater.* **2007**, *6*, 183.
(36) Novoselov, K. S.; Jiang, D.; Schedin, F.; Booth, T. J.; Khotkevich, V. V.; Morozov, S. V.; Geim, A. K. *Proc. Natl. Acad. Sci. U.S.A.* **2005**, *102*, 10451.

(37) Berger, C.; Song, Z.; Li, X.; Wu, X.; Brown, N.; Naud, C.; Mayou, D.; Li, T.; Hass, J.; Marchenkov, A. N.; Conrad, E. H.; First, P. N.; De Heer, W. A. *Science* **2006**, *312*, 1191.
(38) Kim, K. S.; Zhao, Y.; Jang, H.; Lee, S. Y.; Kim, J. M.; Ahn, J. H.; Kim, P.; Choi, J. Y.; Hong, B. H. *Nature* **2009**, *457*, 706.
(39) Viculis, L. M.; Mack, J. J.; Kaner, R. B. *Science* **2003**, *299*, 1361.
(40) Chen, G.; Weng, W.; Wu, D.; Wu, C.; Lu, J.; Wang, P.; Chen, X. *Carbon* **2004**, *42*, 753.
(41) Li, X.; Wang, X.; Zhang, L.; Lee, S.; Dai, H. *Science* **2008**, *319*, 1229.
(42) Hernandez, Y.; Nicolosi, V.; Lotya, M.; Blighe, F. M.; Sun, Z.; De, S.; Mcgovern, I. T.; Holland, B.; Byrne, M.; Gun'ko, Y. K.; Boland, J. J.; Niraj, P.; Duesberg, G.; Krishnamurthy, S.; Goodhue, R.; Hutchison, J.; Scardaci, V.; Ferrari, A. C.; Coleman, J. N. *Nat. Nanotechnol.* **2008**, *3*, 563.
(43) Kim, H.; Abdala, A. A.; Macosko, C. W. *Macromolecules* **2010**, *43*, 6515.
(44) Li, D.; Kaner, R. B. *Science* **2008**, *320*, 1170.
(45) Kim, H.; Miura, Y.; Macosko, C. W. *Chem. Mater.* **2010**, *22*, 3441.
(46) Laaksonen, P.; Kainlauri, M.; Laaksonen, T.; Shchepetov, A.; Jiang, H.; Ahopelto, J.; Linder, M. B. *Angew. Chem., Int. Ed.* **2010**, *49*, 4946.
(47) Linder, M. B.; Szilvay, G. R.; Nakari-Setälä, T.; Penttilä, M. E. *FEMS Microbiol. Rev.* **2005**, *29*, 877.
(48) Henriksson, M.; Berglund, L. A.; Isaksson, P.; Lindstrom, T.; Nishino, T. *Biomacromolecules* **2008**, *9*, 1579.
(49) Jalal Uddin, A.; Araki, J.; Gotoh, Y. *Biomacromolecules* **2011**, *12*, 617.
(50) Zhbankov, R. G.; Firsov, S. P.; Grinshpan, D. D.; Baran, J.; Marchewka, M. K.; Ratajczak, H. *J. Mol. Struct.* **2003**, *645*, 9.
(51) Ferrari, A. C.; Meyer, J. C.; Scardaci, V.; Casiraghi, C.; Lazzeri, M.; Mauri, F.; Piscanec, S.; Jiang, D.; Novoselov, K. S.; Roth, S.; Geim, A. K. *Phys. Rev. Lett.* **2006**, *97*, 187401/1.
(52) Iwamoto, S.; Abe, K.; Yano, H. *Biomacromolecules* **2008**, *9*, 1022.
(53) Johansson, L.-S.; Tammelin, T.; Campbell, J. M.; Setala, H.; Osterberg, M., *Soft Matter* **2011**, *7*, 10917−10924.
(54) Quiocho, F. A. *Biochem. Soc. Trans.* **1993**, *21*, 442.
(55) Lehtiö, J.; Sugiyama, J.; Gustavsson, M.; Fransson, L.; Linder, M.; Teeri, T. T. *Proc. Natl. Acad. Sci. U.S.A.* **2003**, *100*, 484.
(56) Nand, K, V. *Curr. Opin. Struct. Biol.* **1991**, *1*, 732.
(57) Divne, C.; Ståhlberg, J.; Teeri, T. T.; Jones, T. A. *J. Mol. Biol.* **1998**, *275*, 309.